460 nm. Figure 3 shows the power dependence of time-resolved behaviors of another emission in ZnSe thin film at 470 nm. As the excitation power is increased, the faster component of duration less than 1 ps is also increased. This clearly indicates that the fast components are attributed to the stimulated emission from ZnSe under optical-pumping at 400 nm. The time decay and the delay relative to the pumping pulse of the emission maximum of the stimulated emission is changed with the excitation power. These interesting phenomena may be caused by the exciton-exciton scattering inside the thin-film ZnSe.

*Mailing address: 653 W. Hancock #B2, Detroit, Michigan 48201

1. N. Presser, G. Kudlek, J. Gutowski, J. Luminescence 53, 435 (1992).
2. H. Wang, K. S. Wong, I. K. Sou, G. K. L. Wong, Appl. Phys. Lett. 66, 3140 (1995).

CTuL23

High-speed metal-semiconductor-metal photodetector formed by silicon trenches

Jacob Y. L. Ho, K. S. Wong, *Department of Physics, The Hong Kong University of Science and Technology, Clear Water Bay, Kowloon, Hong Kong*

Silicon metal-semiconductor-metal photodetectors (MSM-PDs) are attractive for use in the 0.8-μm wavelength band in optical communication systems due to their much lower cost for very large-scale integration with silicon circuitry. However, the intrinsic disadvantage of silicon is its long absorption depth (~12 μm) at 830 nm, which is the operation wavelength of gallium arsenide lasers, causing a trade-off between responsivity and bandwidth.

The basic concept for high-speed operation of our detector is to ensure carriers are generated in the high-field region. The design structure is shown in Fig. 1(a). Carriers generated in the silicon ridges can be effectively collected by the metal contacts on the sidewalls of the silicon ridges because the electric field here is highly uniform. The depth of the ridge was chosen such that 63% of the 790-nm excitation wavelength light is absorbed. Detector with 10-μm deep interdigitated trenches, having a trench width of 2.5 μm and a spacing of 1.5 μm was fabricated. Due to the process limitation, the actual detector structure is shown in Fig. 1(b). Planar detector with finger width and spacing of 2 μm was also made as a comparison. Details of fabrication steps were omitted here.

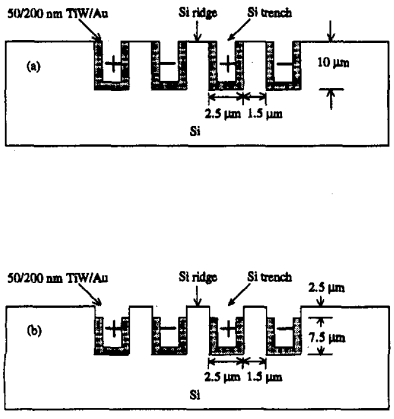

CTuL23 Fig. 1 Cross-sectional view of a MSM-PD formed by silicon trenches. (a) Proposed device structure and (b) actual device structure.

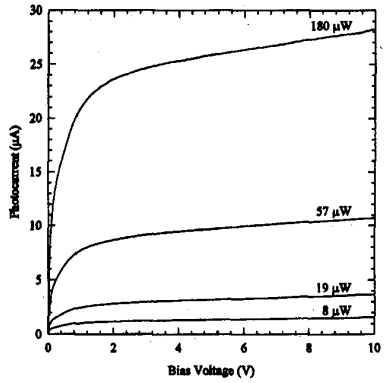

CTuL23 Fig. 2 Current-voltage characteristics of the structured MSM-PD with a trench width of 2.5 μm and a spacing of 1.5 μm at various input optical power. The detector has an active area of 50 μm × 50 μm.

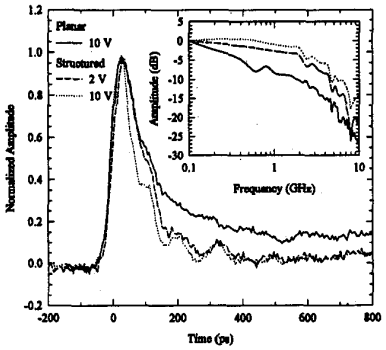

CTuL23 Fig. 3 Impulse response of the structured and planar MSM-PDs under 790-nm optical excitation. The measured pulse widths of the planar detector was 120 ps at 10 V. The structured detector has a pulse width of 98.8 ps and 74 ps at bias of 2 V and 10 V, respectively. Note the absence of diffusion tails for the structured MSM-PD even at low bias. The inset shows the Fourier transform of the impulse response data.

The dc characteristics of the structured silicon detector was characterized at 790-nm wavelength by a HP4145B semiconductor parameter analyzer. The results were plotted in Fig. 2 as a function of applied bias for different input light power levels. The responsivity and external quantum efficiency (QE) of the structured silicon MSM-PD was found to be 0.15 A/W and 24.1% at 10 V (0.13 A/W and 20.3% at 2 V). While that of planar silicon MSM-PD measured under the same bias was 0.24 A/W and 36.9% (0.064 A/W and 10.1% at 2 V). The much higher sensitivity of the structured detector at 2 V indicated that a low bias is sufficient to deplete most of the carriers inside the ridges.

Impulse response of the MSM-PDs was obtained by optical excitation with a 150-fs Ti:sapphire laser at 790 nm (76-MHz repetition rate). The output electrical signal was detected by a 20-GHz digital sampling oscilloscope with a bandwidth limited rise time of 17 ps. Figure 3 shows the output profiles of the structured and planar detectors at different bias. At 10 V, the full-width-at-half-maximum (FWHM) of the structured detector is 74 ps and the 90%–10% fall time is 115 ps (98.8 ps and 196 ps at 2 V). On the other hand, the planar detector has a FWHM of 120 ps and a fall time of 480 ps at 10 V. In addition, it has a long diffusion tail extending to the nanosecond scale. The inset in Fig. 3 shows the Fourier transform of the impulse response data. The structured detector has a −3 dB bandwidth of 2.15 GHz at 10 V (1.25 GHz at 2 V), which is much higher than that of planar detector (240 MHz at 10 V).

In summary, we have demonstrated a brand new structure of MSM detector with 0.15 A/W responsivity at 790-nm wavelength and 2.15-GHz bandwidth at 10-V bias. Compared with conventional planar silicon MSM-PD, this detector was shown to have superior high-speed response and have comparable responsivity with only a simple modification. Most importantly, this detector can operate at 2 V with a slightly less bandwidth (1.25 GHz). Reducing the trench spacing to submicron size can increase the bandwidth at such a low bias. The ease of fabrication together with its high-speed performance at low operating voltages makes the structured MSM detector a strong candidate for optical receivers for short distance optical communication applications.

The authors would like to thank Dr. Curtis Ling in the Department of Electrical and Electronic Engineering for the sampling oscilloscope.

CTuL24

Light extraction efficiency from visible light-emitting diodes

Mikhail Boroditsky, Eli Yablonovitch, *Electrical Engineering Department, University of California–Los Angeles, Los Angeles, California 90095-1594*

Nowadays there is a great demand for high-performance semiconductor light-emitting diodes (LED), which find their application in various branches of modern technology, such as flat panel displays and code division multiplication access communication systems. However, despite very high possible internal

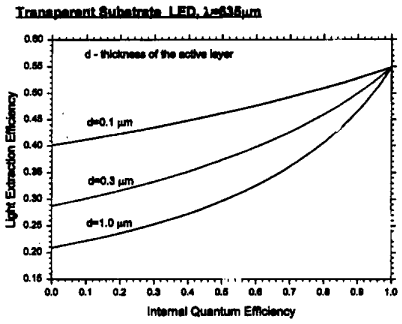

CTuL24 Fig. 1 Light extraction efficiency vs. internal quantum efficiency. Transparent substrate LED, λ = 635 μm.

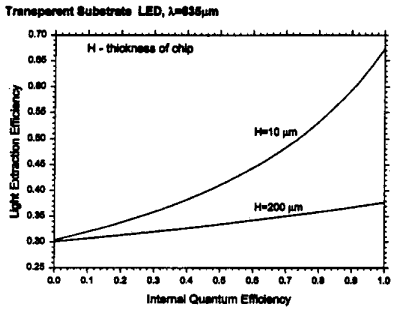

CTuL24 Fig. 2 Light extraction efficiency vs. internal quantum efficiency transparent substrate LED, λ = 635 μm.

quantum efficiency, modern LEDs have relatively low external efficiency because of the narrow escape cone of light from the high refractive index medium. Photon recycling[1] can serve to improve the device performance but is of limited practical applicability. For internal efficiency of 60%, the upper limit of light extraction efficiency is only 10% in a conventional thin film device.

Because escape probability is about 2% per radiating surface, it is a good idea[2] to use all six emitting surfaces of a solid rectangular LED. We introduce a "photonic gas model"[3] for modeling this type of LED. Light extraction efficiency in thick (250 × 250 × 250 μm) transparent substrate LED is a result of competition of light escape from the semiconductor chip, reabsorption in the active layer, and free-carrrier absorption in the bulk. The detailed balance method applied for any part of the "photon gas spectrum" yields spectral escape probabilities. According to our modeling, a very thin active layer can double extraction efficiency to as high as 70%. The calculated dependences of light extraction efficiencies for different thicknesses of the active layer are presented in Fig. 1.

As one can see from Fig. 2, the escape probability of photonic gas increases as the thickness of the wafer is decreased. In this situation the texturing of the top or bottom surface may play an important role. "Natural lithography"[4] is a well explored nanofabrication process that can be used for that purpose. This modelling is confirmed by Monte Carlo simulations. In the future we are going to study light extraction from the LED in details using the Monte Carlo simulations to better understand the distribution of the energy in the device.

In conclusion, visible LED wall-plug efficiency can be more than 50% by making thin-film LEDs with top- or bottom-emitting surface textured in order to provide light randomization.

1. I. Schnitzer, E. Yablonovitch, T. Caneau, T. J. Gmitter, Appl. Phys. Lett. **62**, 131 (1993).
2. F. A. Kish, F. M. Stefanska, D. C. DeFevere, D. A. Vanderwater, K. G. Park, C. P. Kuo, T. D. Osentovsky, M. J. Peanasky, J. G. Yu, R. M. Fletcher, D. A. Steigward, M. G. Craford, Appl. Phys. Lett. **64**, 2839 (1994).
3. E. Yablonovitch, J. Opt. Soc. Am. **72**, 899 (1982).
4. H. W. Deckman, J. H. Dunsmuir, Appl. Phys. Lett. **41**, 378 (1982).

CTuL25

Second-harmonic generation as a nondestructive read-out of information for biological photochromic storage

T. V. Murzina, O. A. Aktsipetrov, A. A. Fedyanin, *Department of Physics, Moscow State University, Moscow 119899, Russia*

Bacteriorhodopsin (bR) is known as one of the promising materials for optoelectronics and some attempts have already been made to build up memory cells on the base of bR-containing systems. The main advantage of the bR molecule is the ability to change its spectral properties under illumination by visible light and dc electric-field application. In this work, we demonstrate that nonlinear-optical method of second-harmonic generation (SHG) with the IR fundamental radiation can be effectively used to determine bR spectral states and suggested as an effective nondestructive read-out for bR-containing systems.

To provide the nonlinear optical read-out, the output of a Q-switched YAG-Nd^{3+} laser at 1064 nm, pulse duration 10 ns, and repetition rate 12.5 Hz was used as fundamental radiation. Optical recording of information was carried out by the cw radiation of an Ar^+ laser in the wavelength range 488–647.1 nm. Oriented bR films 1-μm thick on the silicon substrate were studied. They were prepared from a water suspension of bR-containing purple membranes placed in an orienting electrostatic field. The 100-μm-thick bR films comprised of segments of purple membranes embedded in a poly(vinyl alcohol) matrix (PM-PVA films) were also studied.

Nondestructive read-out of information about bR films spectral state using SHG is demonstrated as the decrease of the SHG intensity $I_{2\omega}$ under the illumination of the bR-PVA film is observed. The changes in $I_{2\omega}$ are caused by the transition of a part of bR molecules into the photoinduced spectral state bR_{412} (where subscript denotes the maximum of the bR intermediate absorption band). The maximal decrease of the SHG intensity corresponds to the case when a dynamical equilibrium sets in between bR_{570} and bR_{412} intermediates. The maximal contrast for $bR_{570} \leftrightarrow bR_{412}$ transition exceeds over 0.8 for the cw radiation intensity $W_i \sim 10$ mW/cm^2 and for all the wavelengths used. Similar behavior was demonstrated by oriented bR films.

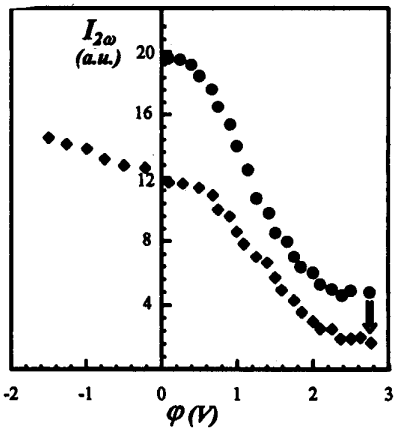

CTuL25 Fig. 1 The SHG intensity $I_{2\omega}$ vs. the applied bias φ with (rhombuses) and without (circles) illumination. The arrow indicates the switching on of the illumination.

Another type of recording of the information in bR films is the dc electric-field application inducing the transition $bR_{570} \rightarrow bR_{630}$. Figure 1 presents the corresponding SHG intensity variations for oriented bR films and in the transmission geometry of the experiment. The maximal contrast of $I_{2\omega}(\varphi)$ dependence is about 0.6. The contrast can be increased to nearly 0.78 as the film is simultaneously illuminated by the cw radiation. It should be noted that dependences $I_{2\omega}(\varphi)$ as well as $I_{2\omega}(W_i)$ were quite reproducible.

We would like to stress that the fundamental radiation at 1064 nm is far from the resonances of the bR molecule. Thus this radiation does not initiate photochromic transformation of bR system. It is testified by the square dependence of the SHG intensity on the intensity of the fundamental IR radiation.

CTuL26

Digital wavelength-multiplexed holographic data storage system

D. Lande, J. F. Heanue, P. Catrysse,* M. C. Bashaw,* L. Hesselink,* *Department of Applied Physics, Stanford University, Stanford, California 94305-4090*

We have implemented, what we believe to be, the first wavelength-multiplexed digital holographic data storage system. The automated storage and retrieval of digital data in an Fe-doped $LiNbO_3$ crys-